Styrene−Butadiene Gradient Block Copolymers for Transparent Impact Polystyrene

Stéphane Jouenne,[†,‡] Juan A. González-Léon,[†,⊥] Anne-Valérie Ruzette,*[,†] Philippe Lodéfier,[§] and Ludwik Leibler[†]

Matière Molle et Chimie, UMR 7167 ESPCI ParisTech-CNRS, ESPCI, 10 rue Vauquelin, 75005 Paris, France, and Total, Groupement de Recherche de Lacq, France

Received June 12, 2008; Revised Manuscript Received October 3, 2008

ABSTRACT: The mechanical behavior of styrene/butadiene triblock copolymers and their blends with high molecular weight polystyrene (PS) homopolymer was studied. Symmetric triblock copolymers with two PS end blocks of equal length (SBS) were compared with asymmetric triblocks with end blocks of different lengths (S1BS2) and with asymmetric triblocks comprising a styrene/butadiene composition gradient in the middle block (S1GS2). The precise molecular architecture of these copolymers and its role on morphology and properties were described elsewhere (*Macromolecules* 2007, *40*, 2432.). Here, immiscible blends of these copolymers with long PS chains are discussed. While solvent casting yields the expected phase separation, melt extrusion produces tough and transparent blends with metastable submicrometer scale dispersions of soft microdomains highly controlled by processing. The particular molecular architecture of gradient asymmetric triblocks significantly improves ductility of these nanostructured blends. The volume fraction of soft microdomains extracted from dynamic mechanical data is identified as a universal parameter that controls tensile behavior of the different blends studied.

I. Introduction

The high strength, optical clarity and low cost of polystyrene (PS) make it one of the most attractive thermoplastic polymers. Most solutions developed to improve toughness of this brittle polymer rely on the controlled dispersion of micrometer-sized particles of a soft polymer like polybutadiene (PB) in the PS matrix.[1,2] PS and PB are immiscible, and their blends phase separate into PS-rich an PB-rich phases. Even though the high shear forces involved during melt processing can break up and disperse a minority PB phase into small droplets, these will most likely coalesce after cessation of shear. The macroscopic PB dispersion that ensues provides little improvement to toughness and yields poor mechanical properties, as is the case for most immiscible polymer blends.[3]

By far the most successful approach to control PB domains and disperse them effectively in a PS matrix is encountered in high impact polystyrene (HIPS). Here, the free radical polymerization of styrene is carried out in presence of PB chains which act as initiators. During the reaction, PS homopolymer chains form as well as PB-*g*-PS graft copolymers. This results in a multiphase material structured at various length scales and that consists of micrometer-sized PB droplets with a complex inner structure of PS inclusions (salami particles) stabilized by styrene/butadiene graft copolymer chains.[4,5] The latter have the dual benefit of reducing coalescence and promoting adhesion of PB particles to the PS matrix.[1,4] Under load, the salami particles act as multiple stress concentrators that nucleate plastic deformation throughout the PS matrix.[6] They also hamper the growth of large crazes that would lead to catastrophic failure. The particular HIPS dispersion offers optimal toughness for limited softening—the typical trade off for rubber toughening. Unfortunately, the rubber particle size and their low index of refraction (n_D(PB) = 1.515 and n_D(PS) = 1.591 at 25 °C[7]) ruin optical transparency of polystyrene.[2] In order to obtain a transparent toughened PS, it is necessary to reduce the soft inclusions size below a few tens of nanometers in a controlled fashion. An attractive solution, originally designed for PS[2,8] and that recently found applications in other thermoplastics, relies on the self-assembly of rubbery/glassy block copolymers in the brittle matrix.[9,10] Block copolymers comprise two or more different polymer chains (blocks) covalently linked together. Incompatibility between the blocks yields molecular-scale (typically a few tens of nm) self-assembly into different mesophases dictated by blocks length and arrangement within the copolymer. The effect of composition, molecular weight and architecture as well as temperature on self-assembly of model block copolymers and their blends with one or two homopolymers has been the subject of numerous studies. Mechanical behavior of rubbery/glassy linear and star copolymers like those of styrene and butadiene or styrene and isoprene have also been widely reported and their deformation mechanisms have been discussed as a function of copolymer morphology and molecular architecture.[11−19] Yet in many applications, the ability to tune mechanical properties of a toughened polymer by changing the ratio of its components in a blend rather than synthesizing a new macromolecule for each specific requirement is highly desirable. S/B block copolymers are thus rarely used pure but in blends with PS where they serve as toughening additives of the brittle matrix. Schwier et al.[14] showed that blending SB diblock copolymers with PS homopolymer increases toughness. They further showed that this increase is directly related to the amount of rubber introduced as well the total molecular weight of the copolymer used.

In a departure from these model systems, however, the copolymers used in practice to toughen PS are characterized by an important degree of molecular disorder, artificially introduced during anionic synthesis through composition gradients along the chain and blending or partial coupling of different copolymers chains.[2,8,20] This level of disorder is apparently key to achieve the desired PS/copolymer blend morphologies and properties in short processing times. The microstructure of the diene block, which controls thermal

* To whom correspondence should be addressed. E-mail: anne-valerie.ruzette@espci.fr.
† Matière Molle et Chimie, UMR 7167 ESPCI ParisTech-CNRS, ESPCI.
‡ Current address: Total, Groupement de Recherche de Lacq, France.
§ Total, Groupement de Recherche de Lacq.
⊥ Current address: CRRA, Arkema, France.

10.1021/ma801327x CCC: $40.75
Published on Web 12/02/2008

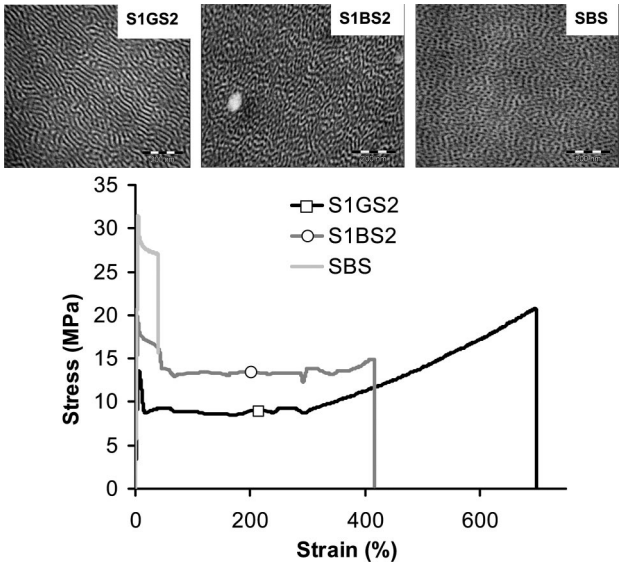

Figure 1. TEM micrographs illustrating the film morphology of S1GS2, S1BS2, and SBS extruded for 3 min at 180 °C and pressed at 170 °C. The bottom graph gives stress−strain curves obtained at room temperature and at a testing speed of 7×10^{-3} s^{-1} on dog-bone shaped specimens cut from these films.

stability and glass transition of the copolymer soft domains, is an important parameter which can be adjusted during synthesis.[20] Likewise, B/S compositional gradients along the chain are introduced by anionic copolymerization of S and B monomers in presence of small amounts of a randomizer such as tetrahydrofuran[2,8] or soluble potassium salts.[20−22] These gradient blocks result in gradual interfaces between soft and hard microdomains which are thought to substantially improve toughness.[23] Several experiments and calculations on composite model systems indeed show that having a gradual change in mechanical properties between two components reduces stress at the interface and improves interfacial adhesion.[24] Although most of the observations on "Functional Graded Materials" (FGM) have been carried out in systems with larger dimensions, it seems reasonable to assume that gradient interfaces between blocks of a copolymer will also enhance mechanical properties. In a recent series of papers,[25−31] Michler and co-workers studied PS-rich S/B linear and star block copolymers of various architectures, some of which contained gradient rubbery middle blocks. Although its effect could not be clearly isolated from other architectural parameters, the gradient block was presented as one of the important features controlling self-assembly[25] and mechanical properties[26] of these copolymers and their blends with polystyrene.[27−31]

In this work, three kinds of triblocks with constant styrene content (∼72 wt % PS) but different molecular structures are considered: the first one is a regular symmetric triblock denoted SBS. The other two are asymmetric in that their PS end blocks have different lengths. One has a pure PB middle block (S1BS2) while the other one has a gradient middle block initially rich in butadiene (S1GS2). These architectural features, namely PS end blocks asymmetry and the gradient middle block, were previously quantified by kinetic modeling of synthesis conversion data and were shown to have a dramatic impact on equilibrium self-assembly and interfacial curvature of these copolymers.[32] SBS indeed adopts a cylindrical morphology expected based on composition, while S1BS2 and S1GS2 are both lamellar. Melt-extrusion performed on a laboratory-scale microcompounder highly disrupts this equilibrium self-assembly which is invariably replaced by bicontinuous-like morphologies lacking long-range order, as illustrated on the top of Figure 1.[32] Yet, tensile specimens cut from extruded and pressed films of these

Table 1. Molecular Characteristics of Materials Studied

	Φ_{PS}[a] (vol %)	M_n[b] (kg/mol)	PDI	τ	morphology
S1GS2	71	121	1.04	0.25	lamellar
S1BS2	71	112	1.08	0.15	lamellar
SBS	77	121	1.18	0.5	cylindrical
PS100H45	100	100	2.11		

[a] Overall styrene volume fractions calculated from the weight fractions determined by ^{1}H NMR and mass densities for PS and PB of 1.05 and 0.95 g/cm^3, respectively. [b] Absolute molecular weights determined by SEC using an internal calibration for these copolymers.

copolymers reveal substantial differences in mechanical behavior among the three pure triblock copolymers despite their identical molecular weights and comparable styrene contents. The stress−strain curves of Figure 1 indeed show a spectacular increase in ductility brought by end-blocks asymmetry and the gradient middle block, as previously reported by Adhikari et al. for similar copolymers.[25] In this work, we further investigate the toughness enhancing effect of these architectural features in *a priori* immiscible blends of these copolymers with high molecular weight polystyrene. The role of melt-processing on the establishment of meta-stable submicrometer scale copolymer dispersions in these blends is discussed. The total volume fraction of dispersed soft microdomains, extracted from low strain dynamic mechanical data, is identified as a key parameter that controls the ultimate strain to break. This soft phase content changes with testing temperature and is highly controlled by copolymer architecture. The boosting effect of a gradient rubbery block is clearly demonstrated.

II. Experimental Methods

Characteristics of the linear S/B triblock copolymers used in this work are listed in Table 1. All copolymers were prepared by batch living anionic polymerization in cyclohexane as described elsewhere.[32] The gradient copolymer S1GS2 was prepared in two steps: a first homopolymerization of pure blocks S1 followed by copolymerization of S and B to yield a gradient initially rich in B and terminated by pure blocks S2 when all B monomers are consumed. Gradient composition profiles along the chain as well as final molecular structure were quantified by modeling conversion data with a simple kinetic model based on the Markov approach.[32] Asymmetry, defined as the ratio τ = S1/S1 + S2 for S1BS2 and S1GS2, is also given in Table 1. All three copolymers were blended with a polystyrene homopolymer, PS100H45, provided by TOTAL Petrochemicals and prepared by free radical polymerization. Its molecular characteristics are also listed in Table 1. This PS contained 4.5 wt % mineral oil, as usually done in practice to improve processing.

Two types of blends were studied. Dilute solutions of the desired amount of copolymer and PS were first prepared in toluene (∼5 wt % solutions) and cast into Teflon molds. Solvent was allowed to evaporate slowly at room temperature for about 2 weeks. The resulting films, ca. 0.3 mm thick, were dried for a few hours under vacuum at 60 °C and then annealed for 48 h at 180 °C. Although not representative of the methods used in practice, solvent casting was chosen to probe the thermodynamic compatibility between PS and the copolymers studied. Direct melt blending was also performed by shearing the copolymer/PS crumbs mixture at 180 °C in a 15 cc DSM twin screw microcompounder equipped with a recirculation valve. After three minutes of blending at a screw rotating speed of 60 rpm, the recirculation valve was opened and the blend was extruded through a cylindrical die, 0.3 cm in diameter, and air-quenched to room temperature. The obtained extruded strands were pressed into films, ∼0.6 mm thick, in a Carver hydraulic press at 170 °C for 20 s. Aluminum spacers were used to control film thickness. Tensile specimens with a gauge length of 25 mm were punched along the extrusion direction from these pressed films.

Uniaxial tensile tests were carried out at 25 and 45 °C and at a strain rate $\dot{\varepsilon}$ of 7×10^{-3} s^{-1} on an Instron 5564 tensile testing

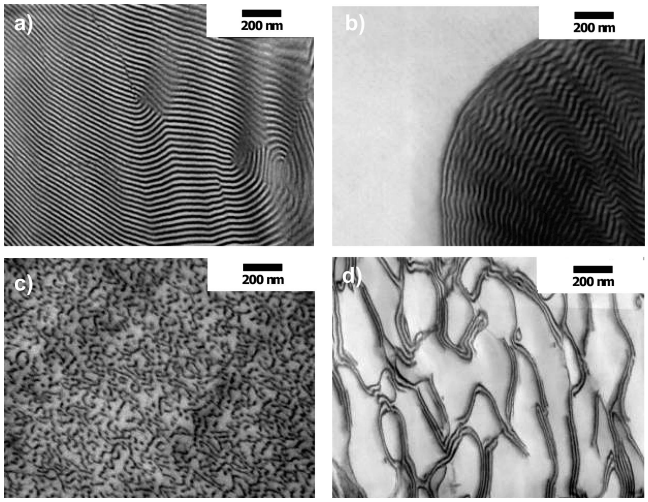

Figure 2. TEM micrographs of solvent cast and annealed films of (a) S1GS2, (b) a 40 wt % blend of S1GS2 in PS100H45, (c) as in part b after being subjected to extrusion for 3 min at 180 °C, (d) as in part c after subsequent annealing at 180 °C for 48 h.

machine. Experiments at 45 °C were performed in an environmental oven with temperature control. At least three specimens were tested for each sample and at each condition. All stress vs strain curves shown below give the engineering stress, i.e., that defined with respect to the initial cross section of the specimen. The small strain tensile behavior of the blends was also measured on a DMA 2980 dynamic mechanical analyzer from TA instruments. Rectangular bars, $L \times l = 20 \times 5$ mm, were machined out of extruded and pressed films and placed in a sample holder operated in tension. Samples were tested under a 0.1% sinusoidal tensile strain applied at a frequency of 1 Hz from −120 to +130 °C at a heating rate of 2 °C/min.

Stability of extruded blend morphologies was studied by recording optical transparency at different temperatures under a Leitz Orthoplan microscope equipped with a 12V halogen lamp and a Mettler FP82 heating stage. Transmitted light intensity was detected using a BPW 34 photodiode. Transmission was reported relative to the initial transparency of the specimen. A nitrogen gas purge was used at all times to avoid degradation of the polymer films.

Sections for transmission electron microscopy (TEM) were ultracryomicrotomed on a Leica Ultracut apparatus at −100 °C. Sections, ca. 50 nm thick, were collected on copper grids prior to exposure to OsO_4 vapor for 45 min. This selectively stains PB segments over PS ones. TEM was carried out on a Zeiss electron microscope operated at 80 kV and equipped with a digital camera from Soft Imaging Systems. Sections from extruded samples were cut perpendicular and parallel to the extrusion direction.

III. Results

III.1. Block Copolymer Dispersion. All solvent cast and annealed blends of PS100H45 with the triblocks listed in Table 1 were phase separated at the macroscopic scale. Parts a and b of Figure 2 illustrate this for the asymmetric gradient triblock S1GS2 (Figure 2a) and its blend with 60 wt % PS100H45 (Figure 2b). The right TEM micrograph reveals the presence of micrometer-sized regions of almost pure copolymer adopting the lamellar morphology of Figure 2a in a matrix of almost pure PS. Such immiscibility was expected based on the high molecular weight of PS100H45 compared with PS blocks of the copolymers.[33,34] These blends are brittle and distinctly opaque as a result of the domain size and differences in index of refraction of PS and PB.

In contrast, blends obtained by melt extrusion were all transparent and substantially tougher than neat PS. Morphologies of these blends differ dramatically from the near equilibrium

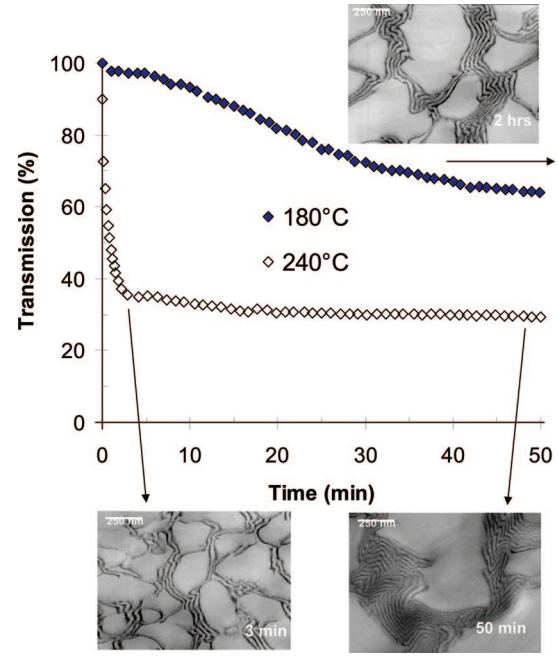

Figure 3. Time-evolution of light transmission and morphology during annealing at 180 and 240 °C for a film of the 40/60 S1GS2/PS100H45 blend.

morphology illustrated above. Figure 2c shows a TEM micrograph of the 40/60 blend of S1GS2 and PS100H45 extruded at 180 °C. Mixing time, i.e., the time spent by the blend in the microcompounder with the recirculation valve closed, was 3 min. After these 3 min, the valve was opened and the blend was extruded through the cylindrical die and subsequently air-cooled. The large copolymer domains observed above are no longer present in this blend. Instead, randomly placed PB nanodomains with no long-range order are homogeneously dispersed throughout the PS matrix. These resemble micelles or broken fragments of lamellar nanodomains whose characteristic size is still controlled by the block copolymer architecture. This obviously nonequilibrium morphology yields transparent materials that, as discussed in more detail below, have good mechanical properties. The impact of mixing time and extrusion temperature as well as the stability of these submicrometer scale dispersions is presented first.

Except in the limit of no recirculation at all, mixing time was found to have no measurable impact on the nature of the dispersion. Temperature, on the other hand, largely controls its size-scale. Although macroscopic phase separation was never obtained, higher extrusion temperatures systematically yielded coarser dispersions. This was attributed to the two following effects: higher melt temperatures mean lower viscosities and thus lower resulting shear forces for mixing. They also result in longer cooling times before freezing below $T_{g,PS}$, giving more time for coalescence of the copolymer dispersion prior to quenching. In what follows, all blends were thus extruded under identical conditions, namely at a melt temperature of 180 °C and after 3 min of mixing. Although not shown here, dispersions entirely similar to that shown in Figure 2c were observed for all copolymers.

As suggested by the contrasting blend morphologies of Figure 2, parts b and c, extrusion produces out of equilibrium dispersions that are trapped upon air-cooling of extruded strands. These spontaneously evolve toward phase separation when reheated above $T_{g,PS}$ in the absence of shear. This is illustrated in Figure 2d for the 40/60 S1GS2/PS100H45 blend annealed under vacuum for 24 h at 180 °C after melt processing. Although macroscopic phase separation is far from complete, well-defined

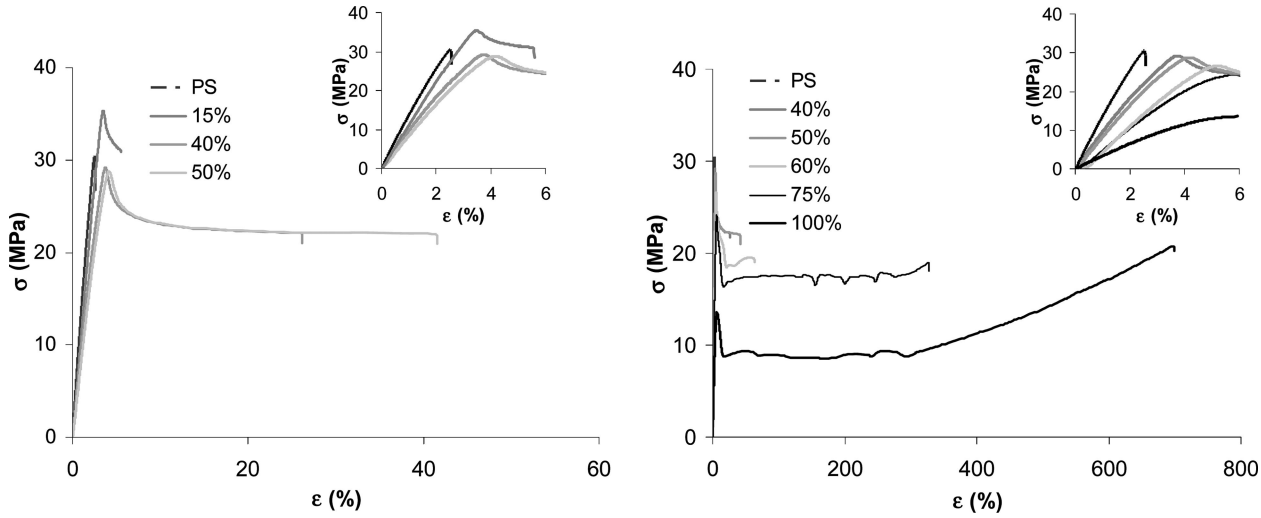

Figure 4. Stress−strain curves of S1GS2/ PS100H45 blends of different compositions. Insets show a zoom on the low deformation part of the curves.

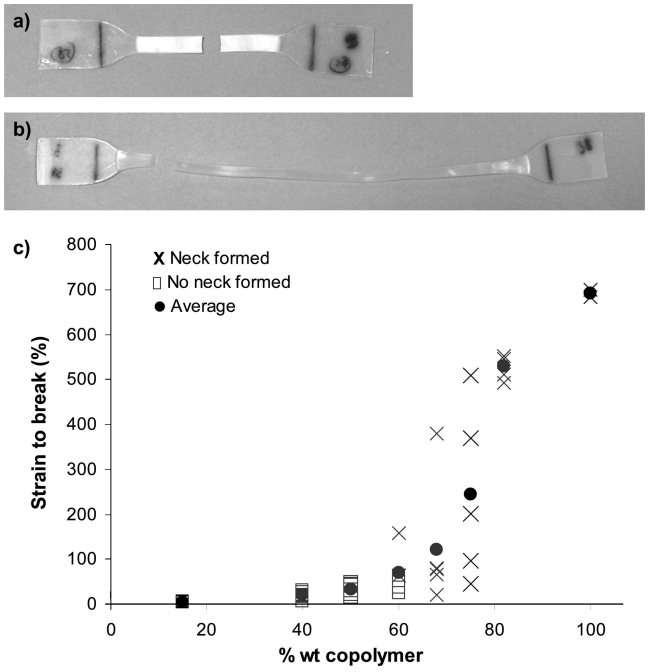

Figure 5. Photographs of tested specimens of S1GS2/PS100H45 blends with (a) 50 wt % and (b) 75 wt % S1GS2. (c) Strain to break as a function of copolymer content for the same blends. Symbols indicate the number of samples that formed a neck during testing (×) compared to those which did not (□).

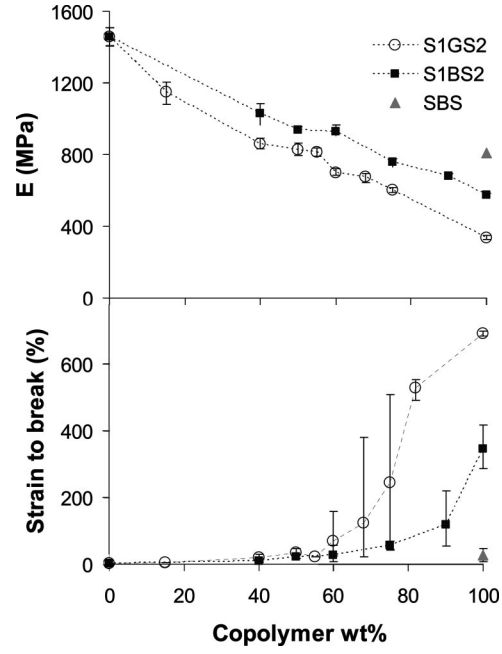

Figure 6. Evolution of Young modulus (a) and strain to break (b) with copolymer content in blends of indicated copolymers with PS100H45.

lamellar regions start to form around pure PS regions. This evolution of morphology is also accompanied by a strong alteration of optical transparency and the sample becomes progressively cloudy. This feature can be used to quantify the kinetics of coalescence and its dependence on temperature by optical microscopy. Figure 3 shows the time evolution of transmitted intensity for an extruded and pressed film of the 40/60 S1GS2/PS blend at two different temperatures. While it takes about 30min to fall below 70% of the original transmittance at 180 °C, it takes less than 5 min to fall below 40% at 240 °C. The obtained morphologies at ∼2 h (180 °C) and at 3 and 50 min (240 °C), respectively, are illustrated as insets on Figure 3. From these results, it is manifest that morphology of these long PS/copolymer blends is largely controlled by kinetics. Processing conditions are thus expected to play an important role on final optical and mechanical properties of these nanostructured materials. While the high shear and elongational forces developed during melt processing are largely able to disperse block copolymers in the long PS homopolymer matrix, these dispersions are only preserved if the blend is rapidly quenched after processing. Similar suppression of macrophase separation by processing was previously reported by Yamaoka for SB/poly(methyl methacrylate) blends[35] and by Adhikari et al. for S/B linear[27,28] and star[29−31] copolymers blended with a PS twice shorter than the one studied here. In the latter studies, however, injection molding was found to produce partially macrophase separated structures and injected tensile specimens were opaque. This is probably due to the different force field exerted on the melt as well as more extensive coalescence upon slow cooling from a higher melt temperature (∼225 °C) than the one used here for extrusion. In the present study, all mechanical measurements were obtained on extruded and air-quenched strands subsequently pressed promptly into films at 170 °C. It was verified that this final step did not alter the dispersion of PB-rich nanodomains in the PS matrix obtained

Table 2. Tensile Properties, T_g's and Soft Phase Content of Pure Copolymers

	E (MPa)	σ_y (MPa)	ϵ_B (%)	$T_{g,soft}$[a](°C)	$T_{g,PS}$[a](°C)	$\phi_{soft,\ 25\ °C}$(%)	$\phi_{soft,\ 45\ °C}$(%)
S1GS2	337 ± 10	13.4 ± 0.2	691 ± 10	−45	108	58	62
S1BS2	576 ± 10	19.8 ± 0.1	346 ± 60	−89	111	40	45
SBS	807 ± 6	31.1 ± 0.5	27 ± 10	−91	112	23	27
PS100H45	1459 ± 40		3.0 ± 0.1		110	0	0

[a] Determined from the maximum of tan δ.

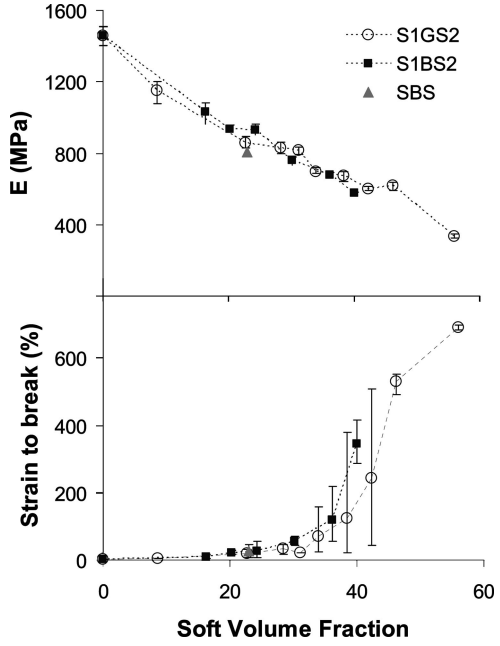

Figure 7. Evolution of young modulus (a) and strain to break (b) with the volume fraction of soft microdomains in blends of indicated copolymers with PS100H45.

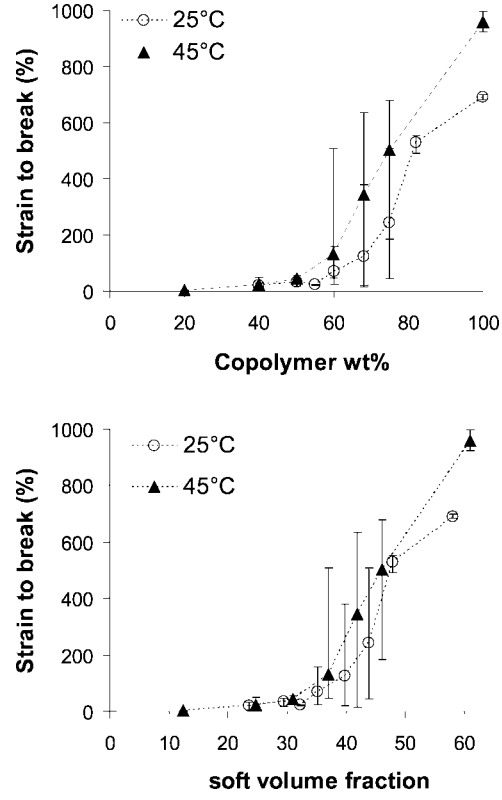

Figure 8. Evolution of strain to break with copolymer content (a) and volume fraction of soft microdomains (b) in blends of S1GS2 with PS100H45 at 25 and 45 °C.

after extrusion (Figure 1). This type of dispersion should be relevant for most sheet and film applications of these blends. Of course, it will be less relevant for thick injected parts for which cooling rate variations across the specimen thickness might result in coarser dispersions in the center and finer ones at the edges. This in turn will substantially alter optical and mechanical properties of injected specimens, not studied here.

III.2. Tensile Behavior of Nanostructured PS/Copolymer Blends. Solvent cast and annealed blends of these copolymers with PS100H45 were all opaque and displayed highly deteriorated properties compared to neat copolymers and PS. In contrast, extruded (nanostructured) blends of PS100H45 with increasing fractions of S1GS2 became increasingly ductile. Figure 4a shows the stress/strain curves of a series of blends containing up to 50 wt % of this copolymer. The addition of 15 wt % S1GS2 (the lowest concentration studied) is already enough to confer a ductile behavior to the brittle PS matrix. This manifests itself in the appearance of a clear yield point and a strain at break substantially higher than that of pure PS. The higher breaking stress of this blend compared to pure PS reflects the brittleness of PS which does not reach its yield point under the testing conditions used here. The strain at break of the blends progressively increases with copolymer content, while elastic modulus and yield strength monotonically decrease. Surprisingly, while the latter both decrease linearly, the change in strain to break is far from linear. This can be seen in Figure 4b which shows the evolution of stress/strain curves of the blends over a larger range of copolymer contents. The strain to break increases dramatically between 60 and 75 wt % copolymer, and this is accompanied by a macroscopically observable change of deformation mechanism. Above 60 wt % copolymer, a drop in tensile stress following the yield point is accompanied by the formation of a macroscopic stable neck, as was observed for the pure copolymers S1BS2 and S1GS2. No whitening occurs except locally at the very last instant before failure. Below 60 wt % copolymer, all blends whiten heavily upon stretching and this whitening is not accompanied by a visible neck formation. This would suggest that cavitation and/or crazing typical for toughened PS is the dominant mechanism at low to intermediate copolymer fractions, while a shear yielding mechanism that allows the formation of a stable neck might be active at higher copolymer fractions. A tested specimen with 50 wt % S1GS2 is shown in Figure 5a. Whitening over the whole gauge length is clearly visible. Figure 5b shows a specimen with 75 wt % S1GS2. The larger strain at break of this blend can be appreciated on the picture, as well as the stable growth of the neck. The observed transition between these two types of behavior is not sharp. At intermediate compositions (60 wt % copolymer for S1GS2/PS blends), part of the specimens tested formed a neck while the rest did not. In fact, the number of specimens not forming a neck systematically decreases as copolymer content increases. The plot in Figure 5c illustrates this by showing the strain to break vs copolymer content for S1GS2/PS blends. The observed behavior (neck or no neck formed) is reported as indicated for each blend composition. Below 60 wt % copolymer, none of the samples formed a neck. At 60 wt %, two out of five did and above 68 wt %, all of them did. This apparent broad transition can also be observed in the relatively large dispersion of strain to break

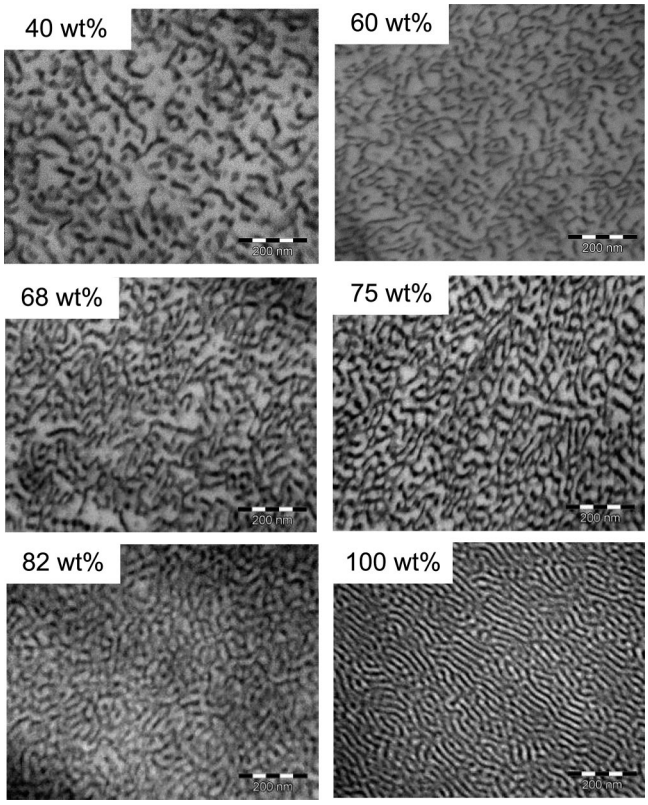

Figure 9. TEM micrographs for a series of blends of PS100H45 with increasing and indicated amounts of S1GS2. All micrographs were obtained on ultrathin sections (maximum 50 nm) to avoid excessive superposition of microdomains in the 2D-projection.

at 68 and 75 wt %. At these concentrations, several specimens failed at low strains even though they formed a neck. By 80 wt % S1GS2, necking became stable, and the dispersion in strain to break is significantly narrower.

Entirely similar trends in mechanical behavior were observed for blends of PS100H45 with S1BS2. Yet, for a given amount of copolymer added to PS, the ductility enhancement achieved with S1BS2 is far inferior to that achieved with S1GS2. Very high strains to break (over 100%) were not achieved in S1BS2 blends until 90 wt % copolymer. This is summarized in Figure 6 which shows the evolution of strain to break and modulus with copolymer content for blends of PS100H45 with S1BS2 and S1GS2. Blends of PS with SBS were not studied since the neat copolymer was not sufficiently ductile by itself. The above-mentioned transition from "ductile" to "highly ductile" materials can be clearly observed for each type of blends. For S1GS2/PS100H45 blends, it occurs around 70 wt % copolymer, while a higher fraction of 90 wt % copolymer is needed with S1BS2. Other tensile properties such as modulus and yield strength of these blends vary linearly with copolymer fraction, as shown in Figure 6b. The curves for S1GS2 and S1BS2 blends have slightly different slopes and differ mostly at higher copolymer compositions where the inherent difference in modulus of the pure copolymers is strongly felt. This observed linear dependence of modulus with composition corresponds well with previous observations by Adhikari et al. on blends of PS with copolymers of similar molecular architecture.[28] Yet, the overall behavior of the blends studied here is significantly different. Their samples only showed very limited deformation (~11%) even for blends containing as mush as 80 wt % copolymer. At this concentration, S1GS2/PS blends have already reached a strain to break of about 400%. This difference might be due to the different processing conditions used to prepare the blends studied by Adhikari and co-workers. As explained above, these were injection molded at high temperatures (~225 °C), which is expected to have a strong impact on the size-scale of copolymer dispersion. This is supported by the observation that some of their blends were cloudy after processing.[28] In addition, intrinsic differences in the molecular characteristics of the PS homopolymer and copolymers studied, such as total molecular weight, individual block lengths and the shape of the gradient middle block—not known for the cited references—might also be responsible for these differences.

IV. Discussion

The results presented above show how two of the three copolymers investigated here can be effectively used to toughen a PS matrix consisting of long homopolymer chains while preserving its optical transparency. This requires melt-blending at high shear rate to overcome the nonzero surface tension between stretched PS blocks and the long PS homopolymer chains used.[36] The surface tension between a grafted layer of symmetric copolymer chains and long homopolymer chains can be estimated according to:[37]

$$\Delta F v/akT \cong 0.926\chi^{1/18}N^{-4/9} \quad (1)$$

where v is the specific monomer volume, a is the average segment size, χ is the Flory−Huggins segmental interaction parameter between the different blocks and N is the polymerization index of copolymer chains. The correct N to be considered here is half the total triblock length, i.e., 740 for S1GS2.[32] For $v_{S/B} = 82$ cm^3/mol, $a = 0{,}65$ nm[38] and an effective χ parameter between PS blocks and S/B gradient blocks previously estimated to be 0.017 at 180 °C,[32] eq 1 yields an estimated surface tension ΔF of about 10^{-4} N/m. Under shear, the smallest theoretical radius of dispersed copolymer particles can then be estimated according to:[39]

$$R \cong \frac{\Delta F}{\eta\dot{\gamma}} \quad (2)$$

where η is the PS matrix viscosity at given T and shear rate $\dot{\gamma}$. At 180 °C and for $\dot{\gamma} \approx 10$ s^{-1} (the estimated shear rate in our twin-screw microcompounder), $\eta_{PS100H45}$ is about 10^4 Pa·s,[40] yielding a theoretical radius R on the order of 10 nm. Clearly, this is the size of most copolymer droplets observed in our extruded blends (Figure 2c). More elongated objects are also visible, which should result from coalescence into copolymer bilayers. Their low concentration indicates that dynamic coalescence during blending is strongly suppressed in these immiscible copolymer/homopolymer blends. Yet, the obtained dispersions are thermodynamically unstable and spontaneously evolve toward macroscopic phase separation when heated above $T_{g,PS}$ in the absence of shear. This has important implications from a processing standpoint since it means that melt temperature and cooling rates largely determine the ultimate morphology and properties.

For the film geometry investigated here, which is very far from equilibrium but common in applications involving such copolymers, highly ductile blends are obtained which are structured at the nanometer scale. Their tensile behavior reveals a nonlinear evolution of strain to break with copolymer content, which is accompanied by a distinct transition in deformation mechanism, from crazing (Figure 5a) to homogeneous shear yielding (Figure 5b) at a critical copolymer concentration which depends on the copolymer molecular architecture. Interestingly, we found that we could directly correlate this behavior with the effective volume fraction of soft microdomains Φ measurable for each blend or copolymer by dynamic mechanical testing. We indeed showed previously that modeling dynamic mechanical data with a Kerner composite equation[41] combined with the Gordon−Taylor equation[42] for T_g could be used to

extract Φ and composition profiles across microdomains of the pure copolymers studied here.[32] To this end, a simplified Kerner equation was used:

$$\Phi(T) = \frac{E_m(T) - E_c(T)}{E_m(T) + \alpha E_c(T)} \quad (3)$$

where E_c and E_m are the pure copolymer and pure PS moduli experimentally measured at T by DMA, and $\alpha = 2(4 - 5\nu_m)/(7 - 5\nu_m)$ where ν_m is the matrix's Poisson ratio, taken to be 0.33. At 25 °C, the temperature at which tensile tests were carried out, DMA data and eq 3 yield as much as 58 vol % soft phase for S1GS2, against 40% for S1BS2 and only 23% for the SBS used here.[43] Clearly, this measure is more relevant than the almost constant PB content to explain the observed differences in modulus, yield strength and strain to break shown in Figure 1 and reported in Table 2 for the neat copolymers.

The volume fraction of soft microdomains for each blend composition studied here can also be determined by modeling dynamic mechanical data. Alternatively, a simple estimate can be obtained by multiplying the fractions listed in Table 2 for each pure copolymers by the blend copolymer content. The evolution of tensile modulus and elongation to break of S1GS2, S1BS2, SBS and their blends with PS are plotted as a function of these estimated soft phase volume fractions in Figure 7. While these properties followed individual curves for each copolymer when plotted as a function of copolymer content (Figure 6), a much more universal trend is now obtained as a function of soft phase fraction. Pure copolymer properties also fit into this curve, indicating that the fraction of soft microdomains is indeed a key parameter that governs mechanical properties of these materials, at least under the testing conditions used. A value of ∼40 vol % can be extracted from Figure 7b as the critical soft phase fraction above which the mechanical behavior of these blends changes from ductile to highly ductile and from crazing to shear yielding.

To further demonstrate the role of the soft phase fraction on mechanical properties of these blends, additional tensile tests were carried out on S1GS2/PS100H45 blends at a slightly higher temperature. Upon heating from T_1 to T_2, an additional fraction of copolymer microdomains and interphase softens, which manifests itself in a reduction of the tensile modulus measured by DMA. The corresponding new fraction of soft microdomains at T_2, Φ_{T_2}, is easily calculated with eq 1. A temperature of 45 °C was chosen for T_2 since it would provide a measurable increment in soft phase volume fraction of the copolymer, from 58 to 62 vol %, while keeping the intrinsic mechanical behavior of the PS matrix unchanged.[44,45] Figure 8a compares the strain to break of S1GS2/PS blends of different compositions at 25 and 45 °C. It can be seen that this small change in temperature induces a shift in the evolution of strain to break with copolymer content of about 10 wt %. In other words, the fraction of copolymer needed to induce a highly ductile behavior is by ∼10 wt % lower at 45 °C. If the strain to break is plotted as a function of soft phase volume fraction, as done in Figure 8b, the curves are only shifted by ∼ 4 vol %, i.e., the increment of soft phase caused by the change in temperature. This further confirms the key role played by soft phase content in these nanostructured blends. It also confirms the existence of a temperature-dependent critical soft phase fraction to obtain shear-yielding and a highly ductile behavior in these blends. Although this falls outside the scope of the present study, it is expected that this fraction will also change with strain rate, loading conditions, and surely even processing conditions.

It is interesting to confront these results with the recent literature on rubber toughened PS. For injected blends of PS and star-shaped asymmetric gradient copolymers, Adhikari et al. indeed reported a very good correlation between ductility and the average PS ligament thickness.[29] The latter corresponds to the average distance between soft (PB-rich) microdomains. The dispersion consisted in highly oriented alternating PS-rich and PB-rich sheets for which an average interlayer distance could be easily calculated. They found a transition from crazing to homogeneous shear-yielding of PS as the PS sheets thickness fell below 30 to 20 nm. This result can be related to recent numerical simulations of the deformation mechanisms of PS, which suggest a brittle to ductile transition below a critical PS ligament thickness of 15 nm.[46] Unfortunately, this average PS ligament thickness or interparticle distance could not be determined for the fine and rather isotropic dispersions studied here and shown in Figure 9 for a series S1GS2/PS blends. The Fourrier transform of these micrographs does not yield a characteristic interparticle distance, nor does SAXS. Yet, close inspection of the morphologies shown in Figure 9 suggests that connectivity of soft microdomains might be an important parameter. Up to 60 wt % block copolymer in the blend, soft microdomains for spherical and wormlike micelles which do not seem connected. Above 68 wt %, i.e., where ductility starts to strongly increase in PS100H45/S1GS2 blends, connectivity becomes evident on TEM micrographs. This suggests that, besides confinement of the PS matrix, percolation of soft microdomains is also necessary to achieve high ductility in the nanostructured blends studied here.

V. Conclusions

The mechanical behavior of immiscible blends of high molecular weight PS homopolymer with linear symmetric (SBS), asymmetric (S1BS2) and gradient (S1GS2) triblock copolymers of styrene and butadiene of constant molecular weight and composition (∼72 wt % PS) was studied. Solvent cast and annealed blends were opaque and indeed showed macroscopic phase separation and deteriorated mechanical behavior. In contrast, extruded sheets of these blends were tough and transparent and displayed fine metastable dispersions of PB-rich microdomains in the PS matrix. These nonequilibrium dispersions are highly dependent on processing conditions and subject to coalescence and macroscopic phase separation upon thermal annealing under static conditions.

The particular molecular architecture of the triblocks studied here, namely PS end-blocks asymmetry (for S1BS2) combined with a gradient middle block (for S1GS2), were shown to be a practical route to impart toughness to these PS-rich copolymers and their blends with PS. The classical SBS of equivalent molecular weight and composition is indeed intrinsically too brittle to toughen PS. Despite its softening effect, the gradient middle block highly contributes to ductility and strains to break of several hundreds percent were measured for blends containing more than 68 wt % gradient triblock copolymer S1GS2. This was accompanied by a distinct change in micromechanism of deformation, from crazing to shear yielding. More than 90 wt % of the asymmetric triblock S1BS2 were necessary to achieve the same behavior in S1BS2/PS blends.

The volume fraction of soft microdomains, as determined by modeling dynamic mechanical data of pure copolymers and blends with a simple Kerner composite equation, was found to successfully correlate with mechanical behavior. Hence, below soft phase fractions of about 40 vol %, ductility is moderate and the blends undergo crazing and extensive whitening upon tensile loading. Above this critical soft phase fraction, the blends become excessively ductile and undergo shear yielding and neck propagation. No whitening occurs in this case. For a given composition, molecular architecture of the copolymer strongly affects the fraction of soft microdomains and thus the mechanical behavior. The largest fraction was obviously achieved for the gradient asymmetric triblock for which S and B monomers are mixed in the longer tapered middle block.

It is tempting to relate the notion of critical soft phase fraction reported here to the critical PS ligament thickness recently predicted by numerical simulations by van Melick et al.[46] and experimentally observed by Adhikari et al.[28,31] for similar though much less ductile blends. Unfortunately, the very fine isotropic dispersions of soft microdomains produced by extrusion do not yield a simple measure of such distance for the blends studied here. The critical fraction of soft microdomains is probably a volumetric equivalent of this distance. It is expected that this critical fraction of soft microdomains will vary with testing speed, temperature, and certainly processing conditions.

Acknowledgment. We are deeply indebted to our colleagues from Total-Petrochemicals, in particular B. Vuillemin who initiated this project, and J. Neelen for helpful discussions. We thank C. Dégoulet and M. Milléquant for their help with SEC analyses and V. Loustalot for her help with the pilot-scale anionic syntheses of block copolymers. The authors thank the UPR5 ESPCI-CNRS TEM group. This work benefited from stimulating discussions with M. Cloître and C. G'sell. We acknowledge financial support from CNRS, ESPCI, and TOTAL.

References and Notes

(1) Henton, D. E.; Bubeck, R. A. In *Polymer Toughening*; Arends, C. B., Ed.; Marcel Dekker: New York, 1996; Chapter 8.
(2) Priddy, D. In *Encyclopedia of Polymer Science and Technology*; John Wiley & Sons: New York, 2006; Vol. 4, p 252.
(3) Utracki, L. A., *Polymer Blends Handbook*; Kluwer Academic Publishers: Norwell, MA, 2002; Vols. 1 and 2.
(4) Echte, A. *Adv. Chem. Ser.* **1989**, *222*, 15.
(5) Fischer, M.; Hellman, G. P. *Macromolecules* **1996**, *29*, 2498.
(6) Donald, A.; Kramer, E. *J. Appl. Polym. Sci.* **1982**, *27*, 3729.
(7) Brandrup, J.; Immergut, E. H.; Grulke, E. A. *Polymer Handbook*, 4th ed.; John Wiley and Sons: New York; 1999.
(8) Knoll, K.; Niessner, N. *Macromol. Symp.* **1998**, *132*, 231.
(9) Ruzette, A. V.; Leibler, L. *Nat. Mater.* **2005**, *4*, 19.
(10) Leibler, L. *Prog. Polym. Sci.* **2005**, *30*, 898.
(11) Morton, M.; McGrath, J. E.; Juliano, P. C. *J. Polym. Sci. Part C* **1969**, *26*, 99.
(12) Fujimura, M.; Hashimoto, T.; Kawai, H. *Rubber Chem. Techol.* **1978**, *51*, 215.
(13) Argon, A. S.; Cohen, R. E.; Jang, B. Z.; Vander Sande, J. B. *J. Polym. Sci., Polym Phys Ed.* **1981**, *19*, 253.
(14) Schwier, C. E.; Argon, A. S.; Cohen, R. E. *Polymer* **1985**, *26*, 1985.
(15) Séguéla, R.; Prud'homme, J. *Macromolecules* **1981**, *14*, 197.
(16) Koltisko, B.; Hiltner, A.; Baer, E. *J. Polym. Sci., Part B: Polym. Phys.* **1986**, *24*, 2167.
(17) Sardelis, K.; Michels, H. J.; Allen, F. R. S. *Polymer* **1987**, *28*, 244.
(18) Sakurai, S.; Sakamoto, J.; Shibayama, M.; Nomura, S. *Macromolecules* **1993**, *26*, 3351 .
(19) (a) Cohen, Y.; Albalak, R. J.; Dair, B. J.; Capel, M. S.; Thomal, E. L. *Macromolecules* **2000**, *33*, 6502. (b) Cohen, R. E.; Thomas, E. L. *Macromolecules* **2003**, *36*, 5265.
(20) Knoll, K.; Fischer, W.; Gausepohl, H.; Koch, J.; Wunsch, J.; Naegele, P. US Patent 6,593,430, July 15 **2003**.
(21) Wofford, C. F.; Hsieh, H. L. *J. Polym. Sci., Part. A-1* **1969**, *7*, 461.
(22) (a) Smith, S. D.; Ashraf, A. *Polym. Prepr.* **1993**, *34*, 672. (b) Smith, S. D.; Ashraf, A. *Polym. Prepr.* **1994**, *35*, 466.
(23) Asai, S. *Polym. Prepr.* **1996**, *37*, 706.
(24) Tilbrook, M. T.; Moon, R. J.; Hoffman, M. *Compos. Sci. Technol.* **2005**, *65*, 201.
(25) Adhikari, R.; Michler, G. H. *Prog. Polym. Sci.* **2004**, *29*, 949.
(26) Adhikari, R.; Godehardt, R.; Lebek, W.; Goerlitz, S.; Michler, G. H.; Knoll, K. *Macromol. Symp.* **2004**, *214*, 173.
(27) Huy, T. A.; Adhikari, R.; Lüpke, T. H.; Michler, G. H.; Knoll, K. *Polym. Eng. Sci.* **2004**, *44*, 1534.
(28) Adhikari, R.; Huy, T. A.; Henning, S.; Michler, G. H.; Knoll, K. *Colloid Polym. Sci.* **2004**, *282*, 1381.
(29) Michler, G. H.; Adhikari, R.; Lebek, W.; Goerlitz, S.; Weidish, R.; Knoll, K. *J. Appl. Polym. Sci.* **2002**, *85*, 683.
(30) Ivankova, E. M.; Adhikari, R.; Michler, G. H.; Weidish, R.; Knoll, K. *J. Polym. Sci. Polym. Phys. Ed.* **2003**, *41*, 1157.
(31) Adhikari, R.; Michler, G. H.; Goerlitz, S.; Knoll, K. *J. Appl. Polym. Sci.* **2004**, *92*, 1208.
(32) Jouenne, S.; González-León, J. A.; Ruzette, A. V.; Lodefier, P.; Tencé-Girault, S.; Leibler, L. *Macromolecules* **2007**, *40*, 2432.
(33) Leibler, L. *Makromol. Chem., Macromol. Symp.* **1988**, *16*, 1.
(34) Semenov, A. N. *Macromolecules* **1993**, *26*, 2273.
(35) (a) Yamaoka, I. *Polymer* **1995**, *36*, 3359. (b) Yamakoa, I. *Polymer* **1996**, *37*, 5343. (c) Yamakoa, I. *Polymner* **1998**, *39*, 1765.
(36) Leibler, L.; Mourran, A. *MRS Bull.* **1997**, *22*, 33.
(37) Leibler, L.; Ajdari, A.; Mourran, A.; Coulon, G.; Chatenay, D. In *Ordering in Macromolecular Systems*; Teramoto, A., Kobayashi, M., Norisuje, T., Eds.; Springer-Verlag: Berlin; 1994; pp 301−311.
(38) Based on molar volumes of 100 and 60 cm^3/mol for S and B, respectively, and statistical segment lengths of 0.67 and 0.63 nm for S and B units, respectively.
(39) Wilkinson, A. N.; Ryan A. J. *Polymer Processing and Structure Development*; Kluwer Academic Publishers: Dordrecht, The Netherlands, Boston, MA, and New York; 1999; Chapter 3; p 207.
(40) Graessley, W. W.; Glasscocic, S. D.; Crawjey, R. I. *Trans. Soc. Rheol.* **1970**, *14*, 519.
(41) Kerner, E. H. *Proc. Phys. Soc. London, Sect. B* **1956**, *69*, 808.
(42) Gordon, M.; Taylor, J. S. *J. Appl. Chem.* **1952**, *2*, 493.
(43) The architecturally symmetric triblock SBS used here is not the same as the one discussed in ref 32, which only contained 74 vol % PS. Both copolymers adopt a cylindrical morphology under equilibrium conditions.
(44) Berger, L. L.; Kramer, E. J. *Macromolecules* **1987**, *20*, 1980.
(45) Donald, A. M. *J. Mater. Sci.* **1985**, *20*, 2630.
(46) Van Melick, H. G. H.; Govaert, L. E.; Meijer, H. E. H. *Polymer* **2003**, *44*, 457.

MA801327X